

# The alloying mechanisms of Re, Ru in the quaternary Ni-based superalloys $\gamma/\gamma'$ interface: A first principles calculation

Yun-Jiang Wang<sup>a,\*</sup>, Chong-Yu Wang<sup>a,b,c</sup>

<sup>a</sup> Department of Physics, Tsinghua University, Beijing 100084, PR China

<sup>b</sup> The International Center for Materials Physics, Chinese Academy of Sciences, Shenyang 110016, PR China

<sup>c</sup> China Center of Advanced Science and Technology (World Laboratory), P.O. Box 8730, Beijing 100080, PR China

Received 5 November 2007; received in revised form 6 January 2008; accepted 7 January 2008

## Abstract

The site preference of Re, Ru on the  $\gamma/\gamma'$  interface and their influence on the partitioning behaviors of W, Mo in the  $\gamma$  and  $\gamma'$  phase have been investigated by DMol3 calculation. The transfer energy results show that both Re and Ru exhibit a weak Ni site preference. When Re substitutes Ni on the  $\gamma/\gamma'$  interface, it is found a reverse partitioning behavior of W, while the partitioning behavior of Mo was not affected. In contrast, Ru's substitution for Ni on the interface does not affect the partitioning behaviors of W, Mo, which is in agreement with experimental results. In addition, the different interface strengthening mechanisms for Re and Ru are investigated by the electronic structure analysis of the Mulliken population, the impurity-induced charge redistribution and the partial density of states. Results show that the alloying strengthening effect of Re is mainly due to the direct bonding of Re and the host atoms. Whereas, the addition of Ru is effective for improving the phase stability of Ni-based superalloys. © 2008 Elsevier B.V. All rights reserved.

PACS: 71.20.Be; 71.20.Lp; 61.50.Lt; 62.20.-x

Keywords: Ni-based superalloys; Interface; Site preference; Strengthening; Partitioning

## 1. Introduction

Ni-based single-crystal (SC) superalloys are widely used for turbine blades and vanes in modern aero-engines as promising high-temperature structural materials because of their remarkable mechanical properties. The typical microstructure of such superalloys is a high fraction of cuboidal  $\gamma'$  phase precipitates coherently embedded in the  $\gamma$  matrix phase. It is the  $\gamma'$  phase that is largely responsible for the elevated-temperature strength of the material and its incredible resistance to creep deformation. Meanwhile, the vast interfacial area between  $\gamma$  and  $\gamma'$  is of great importance for the overall performance of superalloys [1]. The Ni-based SC superalloys are categorized into four generations according to the amount of Re additions. Particularly, the third generation contains approximately 6 wt.% Re, which is proven to be a key refractory element responsible for the improvement of mechanical properties of SC superalloys [2–4]. However, the refractory elements such as Re have a severe drawback that they

may tend to form topologically close-packed (TCP) phases. The precipitation of these refractory-rich TCP is detrimental to the turbine blades material because of the depletion of the solid solution strengthening elements. Therefore, recent studies focus on the fourth generation SC superalloys which have much better mechanical properties and microstructural stability with Ru addition [5,6]. Ru is proven to be an effective element that can suppress the formation of TCP phases in superalloys [6,9,28]. Compared with the second and third generation SC superalloys, the fourth generation, which is characterized by partially replacing Re by Ru, clearly exhibits improved oxidation and corrosion resistance, remarkably higher creep strength as well as an inhibited inclination to the harmful TCP precipitation phases [10].

Both the  $\gamma$  and  $\gamma'$  phase in SC superalloys have a fcc structures with very similar lattice parameters, which is 3.52 Å for fcc Ni and 3.573 Å for  $L1_2$  Ni<sub>3</sub>Al [7]. The  $\gamma$  phase forms the matrix in which the  $\gamma'$  precipitates in a cube–cube orientation relation with the  $\gamma$ . This means that both edges of the two phases are exactly parallel to each other. In other words, when the precipitate size is small, the  $\gamma'$  phase is coherent with the  $\gamma$  in the [001] direction. The coherent structure of

\* Corresponding author.

E-mail address: wangyunjiang05@mails.tsinghua.edu.cn (Y.-J. Wang).

SC superalloys interface is important as it ensures a lower  $\gamma/\gamma'$  interfacial energy, the global minimization of which is the very mechanism of precipitate coarsening. As a result, a coherent or semi-coherent interface makes the microstructure stable, a property which is useful for elevated temperature applications. In the present work, the strengthening mechanisms of Re and Ru are investigated by adopting coherent models, which are reasonable according to the related theoretical and experimental work [8,9].

Re, Ru are the typical additions in the fourth generation SC superalloys, so it is naturally required for people to investigate the different mechanisms of alloy strengthening. It is widely accepted that the mechanism of strengthening due to Re addition lies in the fact that the refractory element Re not only partitions more strongly to the  $\gamma$  matrix [11,12], but also clusters on the  $\gamma/\gamma'$  interface, thus preventing the coarsening of alloying strengthening phase  $\gamma'$ ; whereas alloys containing additions of Ru were shown to exhibit significantly improved high-temperature creep properties due to the absence of the TCP phases, so that the refractory alloying additions remain at the  $\gamma/\gamma'$  interface, and eventually provide a high degree of solid solution strengthening [6]. In a word, the Ru additions in Ni-based superalloys reverse the partitioning behavior of refractory elements such as W, Re, Cr, Mo, causing them partition to the  $\gamma'$  phase instead of the  $\gamma$  phase [13]. Although there is lots of work investigating the different fundamental alloying strengthening mechanisms of Re and Ru, to our knowledge, they are still unclear, especially in the level of electronic structure.

Recently, experiments have shown that in the quaternary SC alloys Ru does not have the desired “reverse partitioning” effect on W, Mo [14]. On the other hand, Re seems to have a repartitioning effect on W, making W partitions more strongly to  $\gamma'$  phase, but Mo is not affected [14]. Nevertheless, deeper understanding of this phenomenon would require knowledge of extensive atomistic calculation. Most work in this field focuses on the  $\gamma'$  phase, where Re prefers the Al site [15], whereas Ru does not have a commonly accepted site preference. Recently, there exists a consistent result that Ru substitutes an Al site in the  $\gamma'$  phase [16,17], and some theoretical works illustrate that Ru's site preference is Ni [18–20]. In order to understand the Re, Ru strengthening effect on host atoms and the added elements W, Mo, the Re, Ru site preference on the  $\gamma/\gamma'$  interface should be firstly determined. Because of the different atom environment in pure  $\gamma'$  and the  $\gamma/\gamma'$  interface, a new site preference of Re and Ru may probably be derived on the  $\gamma/\gamma'$  interface. As an attempt to better explain the different alloying effects of Re and Ru to refractory elements, W(Mo) are doped into the  $\gamma$  and  $\gamma'$  phase, respectively. The difference originating from Re and Ru addition on the interface are compared, and the different alloying mechanisms of Re, Ru in the quaternary Ni-based SC superalloys are investigated. The quaternary superalloys are Ni–Al–Re(Ru)–W(Mo) with Re(Ru) on the interface and W(Mo) in the pure  $\gamma$  or  $\gamma'$  phases. From the energetics and electronic structure analysis of Re and Ru in the  $\gamma/\gamma'$  interface clusters with refractory elements W and Mo, a concrete insight are given into the different alloying mechanisms of Re and Ru.

## 2. Method and computational model

All structures optimizations and total energy calculations reported in the present work are performed using DMol3 [21,22] molecular cluster approach based on density functional theory. In general, it is very convenient to use a cluster model to explore the electronic properties of systems, especially with local defects. Therefore, the DMol molecular cluster approach has been used to analyze the orbital electron occupations. The double numerical basis set for all the atoms with an effective core potentials (ECP) [23,24] as an alternative to all electron calculations have been adopted, in which the valance s, p, d orbitals for all the elements in our calculation are included. The PBE version of the generalized gradient approximation (GGA) [25] is used for the electron exchange and correlation. The convergence criteria for the charge density of self-consistent iterations was set to  $10^{-6}$ , which allows the binding energy to converge to  $10^{-6}$  Ry. Since the magnetic interaction energy makes only a small contribution to the binding energy [26], all DMol calculations are spinrestricted. In the present research, the transfer energy given in our calculations gives the site preference information for Re and Ru on the  $\gamma/\gamma'$  interface; the binding energy, difference charge density, Mulliken orbital population and partial density of states are given in details to analyze the different alloying effect of Re(Ru) on the refractory element W(Mo), especially on the their partitioning behavior.

Two 87-atom cluster models are employed in our calculations in which the center is either an Al or a Ni atom, shown in Figs. 1 and 2. They consist of an upper  $\text{Ni}_3\text{Al}$  region and a lower Ni region, representing the  $\gamma$  and  $\gamma'$  matrix respectively in the Ni-based SC alloys. A transition layer of Ni exists between the two regions, which can be regarded as the either the lowest plane of the  $\text{Ni}_3\text{Al}$  region or the highest plane of the Ni region. Here this transition layer containing atom labeled by 3 are defined and as the uppermost plane of lower Ni region, and the layer contains the central atom labeled by 1 as the lowest plane of the  $\text{Ni}_3\text{Al}$  region. Thus both of the two models contain four layers of the  $\gamma'$  phase and three layers of the  $\gamma$  phase. The Ni atoms labeled by 2 and 3 are the Ni atom sites which are substituted by W(Mo) atoms in the quaternary Ni–Al–Re(Ru)–W(Mo) Ni-based SC superalloys. Atoms 2 and 3 locate in the  $\gamma'$  and  $\gamma$  phase, respectively. The reason why we choose  $2 \times 2 \times 3$  supercell-like clusters instead of  $2 \times 2 \times 2$  ones is that the more accurate information is required across the  $\gamma/\gamma'$  interface as we study the effect of Re, Ru on the partitioning behavior of W and Mo. The  $\gamma/\gamma'$  interface without any substitution by Re(Ru) on the interface and W(Mo) in the pure  $\gamma$  and  $\gamma'$  phases separately are used as baselines for the comparison of Re(Ru), W(Mo) substitution in the quaternary Ni-based SC superalloys. The lattice constant of the individual cluster is the same according to the assumption of complete coherence. The two coherent cluster interface models are used to give the site preference of Re, Ru on the interface. With the result, all the following calculations are just based on the reasonable site preference models. Furthermore, an effort can be made to study the alloying strengthening mechanisms of Re and Ru by comparing the effect on the partitioning behavior of refractory elements W and Mo, and then to demonstrate the

experimental results that Re makes W behave a “reverse partitioning”, but Mo is not the case. However, Ru does not affect the partitioning behavior of both W and Mo.

### 3. Result and discussion

#### 3.1. The equilibrium lattice parameter of the coherent interfacial model

The lattice parameters of the two phases are equal because of the coherence assumption. The lattice parameters for the two coherent models shown in Figs. 1 and 2 are firstly determined by performing a series of total energy calculations using different lattice parameters from 3.20 Å to 4.00 Å. Fig. 3 shows the calculated binding energies  $E_b$  (defined as the difference between of the interactive atom system and that of the free atom system) as functions of the lattice parameters for the pure  $\gamma/\gamma'$  interface. The calculated lattice parameters of both the two cluster models centering on Al and Ni atoms are 3.49 Å corresponding to the lowest binding energy. Compared to the lattice parameters of the pure Ni (3.52 Å) and the pure  $\text{Ni}_3\text{Al}$  (3.573 Å), it is a little smaller.

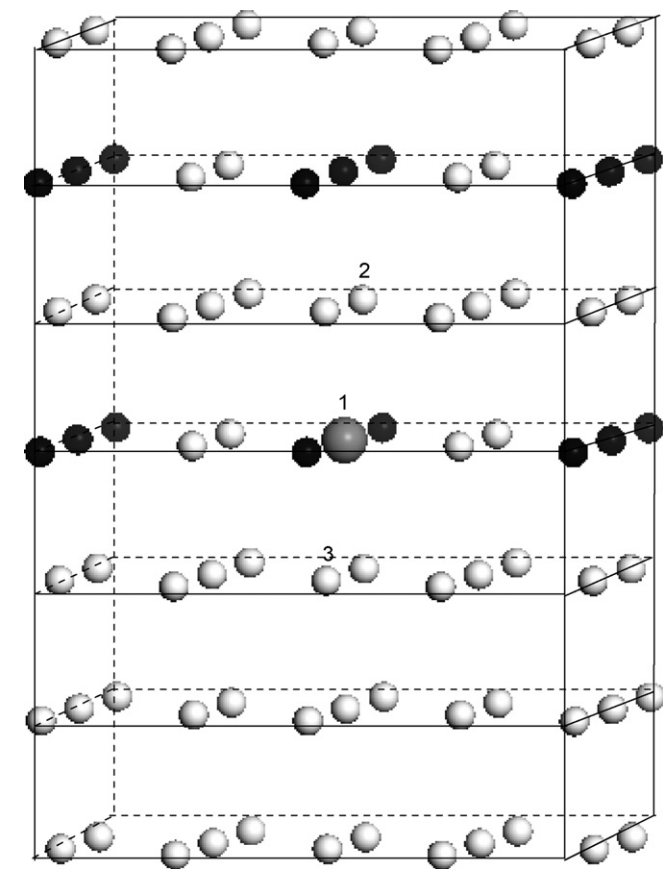


Fig. 1. The 87-atom cluster model of the  $\gamma/\gamma'$  interface centering at an Al atom. The small white and black balls denote a Ni atom and an Al atom, respectively. The central larger grey atoms labeled by the Arabic numeral 1 is Al(Re,Ru,Vac) atom. Two NN Ni atoms across the interface are labeled by 2 and 3, in the  $\gamma$  and  $\gamma'$  phases separately.

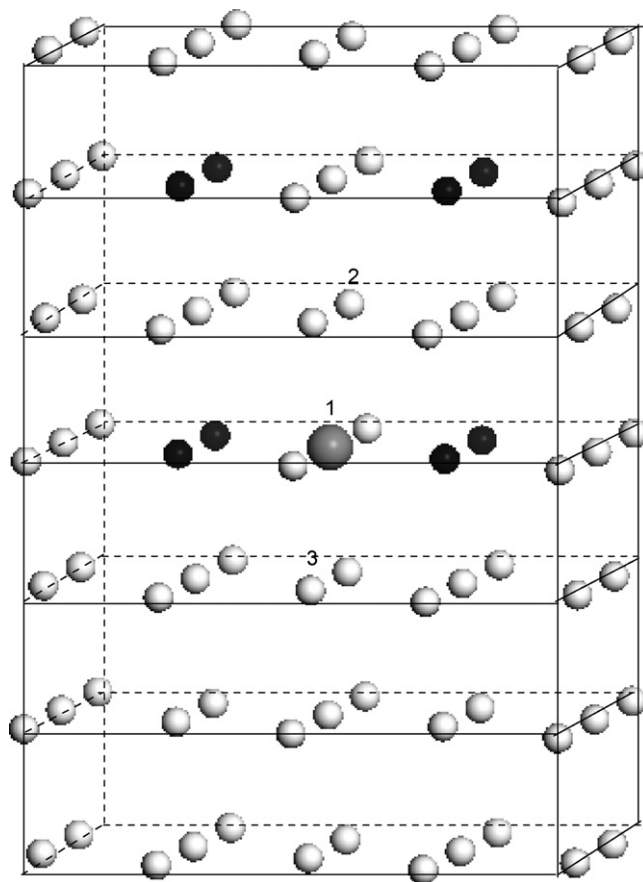


Fig. 2. The 87-atom cluster model of the  $\gamma/\gamma'$  interface centering at a Ni atom. The small white and black balls denote a Ni atom and an Al atom, respectively. The central larger grey atoms labeled by the Arabic numeral 1 is Al(Re,Ru,Vac) atom. Two NN Ni atoms across the interface are labeled by 2 and 3, in the  $\gamma$  and  $\gamma'$  phases separately. They are substituted by W(Mo) in the following calculation.

#### 3.2. Site preference of alloying elements Re and Ru

The main task of the present work is to investigate the effect of Re and Ru on the partitioning behaviors of the refractory ele-

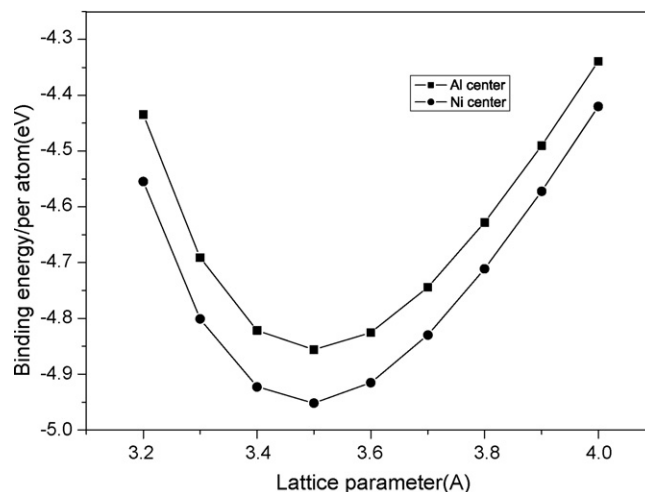


Fig. 3. The calculated binding energy of the pure  $\gamma/\gamma'$  interface. Al center and Ni center correspond to the systems shown in Figs. 1 and 2, respectively.

Table 1

The binding energy (in eV) of the  $\gamma/\gamma'$  system centering at Al atom with and without the presence of the Re(Ru,Vac) atom

System	Binding energy (eV)	$\Delta E$
Ni <sub>3</sub> Al(Al centered)	−676.64	
Ni <sub>3</sub> (Al,Re)	−679.65	3.01
Ni <sub>3</sub> (Al,Ru)	−680.85	4.21
Ni <sub>3</sub> (Al,Vac)	−672.06	−4.58

$\Delta E$  denotes the difference in the binding energies between the interface with the Re(Ru,Vac) substitution and the pure  $\gamma/\gamma'$  interface system centering at an Al atom.

ments W and Mo. To achieve this goal, Re and Ru are doped to the  $\gamma/\gamma'$  interface, and the substitution behavior of Re and Ru on the interface should be known in order to specify correctly the Re and Ru alloying effect on W and Mo. Many researches in this field focus on the site preference of Re and Ru in the pure Ni<sub>3</sub>Al phase, whereas our work is on the coherent  $\gamma/\gamma'$  interface. Taking this different interfacial environment into consideration, a new site preference of the Re and Ru may be given on the interface. The central Al atom in Fig. 1 and Ni atom in Fig. 2 are firstly substituted by a Re or Ru atom or a vacancy and a DMol relaxation calculation is performed. The chemical compositions of the pure Ni<sub>3</sub>Al phases, i.e. Ni<sub>3</sub>Al(Al centered), Ni<sub>3</sub>(Al,Re), Ni<sub>3</sub>(Al,Ru), Ni<sub>3</sub>(Al,Vac), are used to label the total  $\gamma/\gamma'$  interfaces, as shown in Fig. 1. The same method is used to denote the systems related to the coherent models in Fig. 2, whose central atom is Ni, the corresponding symbols are Ni<sub>3</sub>Al(Ni centered), (Ni,Re)<sub>3</sub>Al, (Ni,Ru)<sub>3</sub>Al, (Ni,Vac)<sub>3</sub>Al. All the atoms are allowed to relax in accordance with the forces acting on them except the outmost ones. The outmost layers are kept fixed in order to guarantee the reasonable configuration of the  $\gamma/\gamma'$  interfaces. With the relaxed configurations, the binding energies of the interface systems centering at Al and Ni atom, and the systems with Re or Ru or vacancy substitutions on the interface are calculated. The results are presented in Tables 1 and 2.

It is interesting to find that with the Re and Ru substitution for Al atom, the binding energy of the systems is lower. When Re (Ru) atom occupies an Al site, the binding energy decreases by as much as 3.01 eV (4.21 eV). Both of the two substitutions can decrease the binding energy and result in the improvement of microstructure stability, and Ru appears to give a better alloying stability effect. When a Ru atom occupies a Ni site, the binding energy decreases by 0.48 eV; however, for a Re atom substitution for Ni, it increases by 0.89 eV. The derived result is consistent with known fact that Ru is determined to be a critical element for

Table 2

The binding energy (in eV) of the  $\gamma/\gamma'$  system centering at Ni atom with and without the presence of the Re(Ru,Vac) atom

System	Binding energy (eV)	$\Delta E$
Ni <sub>3</sub> Al(Ni centered)	−716.00	
(Ni,Re) <sub>3</sub> Al	−715.11	−0.89
(Ni, Ru) <sub>3</sub> Al	−716.48	0.48
(Ni,Vac) <sub>3</sub> Al	−707.35	−8.65

$\Delta E$  denotes the difference in the binding energies between the interface with the Re(Ru,Vac) substitution and the pure  $\gamma/\gamma'$  system centering at a Ni atom.

the stabilization of the  $\gamma/\gamma'$  microstructure with respect to TCP phase formation. However, too much Re results in the formation of TCP phase and the instability of Ni-based SC superalloys [27,28]. These results also imply that Re and Ru both have the possibility of occupying either an Al site or a Ni site, therefore, another method is adopted to determine the site preference of Re and Ru in the interface.

The transfer energy [15,29] is used in our present work to judge the site substitution behavior of a Re(Ru) atom on the  $\gamma/\gamma'$  interface. The transfer energy is defined as the energy required to move a single Re(Ru) atom from a Ni site to an Al site. Based on the magnitude and the sign of the transfer energy, the site preference of Re and Ru on the interface can be correctly given. It is easy to notice that the defined transfer energy here has something to do with the perfect cluster interface model and the interface system with a vacancy. For the sake of simplicity, the chemical composites of the  $\gamma'$  (Ni<sub>3</sub>Al) phase are still used to denote the whole  $\gamma/\gamma'$  interface containing both the  $\gamma$  and the  $\gamma'$  regions, namely the transfer energy of a substitutional atom (taking Re for example) on the  $\gamma/\gamma'$  interface is defined as

$$E_{\text{tran}}^{\text{Re}} = \{E_b[\text{Ni}_3(\text{Al}, \text{Re})] - E_b[\text{Ni}_3(\text{Al}, \text{Vac})]\} - \{E_b[(\text{Ni}, \text{Re})_3\text{Al}] - E_b[(\text{Ni}, \text{Vac})_3\text{Al}]\} \quad (1)$$

where  $E_b[\text{Ni}_3(\text{Al}, \text{Re})]$  is the binding energy of the Ni<sub>3</sub>(Al,Re)/Ni interface system, and  $E_b[\text{Ni}_3(\text{Al}, \text{Vac})]$  is the binding energy of the vacancy (no atom in the center) Ni<sub>3</sub>(Al,Vac)/Ni interface system, and so on. The definition of the transfer energy by moving a Ru from a Ni site to an Al site has the similar expression. By our calculation, the transfer energies are 0.18 eV and 0.35 eV for Re and Ru, respectively. These small positive transfer energies indicate that both Re and Ru atoms on the  $\gamma/\gamma'$  interface have a weak Ni site preference. Our result for the Re site preference of the interface region is the same as Peng et al. [30]. To our knowledge, the site preference of Ru is still unclear, experimental work supports an Al site preference in the pure Ni<sub>3</sub>Al phase [16], whereas the theoretical researches show a Ni site preference [19,20]. It is easy to point out that the site preference of an atom on the interface may be totally different from a pure  $\gamma'$  phase case due to the different environment between the pure Ni<sub>3</sub>Al phase and the Ni<sub>3</sub>Al/Ni interface. Therefore, after the site preference of Re and Ru is reliably determined, the different alloying effects of Re and Ru on the  $\gamma/\gamma'$  interface can be further compared. In the following calculations, the effect of Re and Ru on the partitioning behavior of W and Mo are focused. Since the Ni atomic site is the preferable one for both Re and Ru on the interface, our following calculations in the present work are based upon the interface model centering at a Ni atom shown in Fig. 2.

### 3.3. The influence of Re, Ru on the partitioning behavior of refractory elements W, Mo

#### 3.3.1. Binding energy

W and Mo are two important refractory elements added as solid-solution strengtheners in the Ni-based SC superalloys.



They are extremely potent in enhancing the strength and creep performance of alloy. However, there are limits to the concentrations of such elements in that too many of them tend to promote microstructural instability that leads to the rapid formation of refractory-rich topological-close-packed (TCP) precipitates. These deleterious phases remove the refractory solid solution strengthening elements from the constituent  $\gamma/\gamma'$  phases, which results in the rapid degradation of creep properties as TCP phases occurs within the microstructure. Unluckily, there are no simple patterns for the critical concentrations of such elements. Re and Ru are the typical alloying strengthening elements in the fourth generation SC superalloys, but their alloying strengthening mechanisms are not thoroughly understood. Ru was reported as an element to reverse the partitioning behavior of refractory elements in the  $\gamma$  and  $\gamma'$  phases [34]. As is well known, it is the matrix composition which controls the onset of precipitation. By reverse partitioning, the refractory elements in the  $\gamma$  phase is pushed into the  $\gamma'$  phase, thus lowering the refractory elements in the  $\gamma$  and delaying instability. This is the strengthening effect of Ru. Meanwhile, Re is reported to have an effect on repartitioning behavior of W. As we know, our present work is the pioneering effort to elucidate the effect of Re and Ru on the partitioning behaviors of W and Mo from the electronic structure point of view. A detailed analysis of the binding energy, the Mulliken population, the charge difference distribution and partial density of states meet this aim.

Two geometrical symmetric atomic sites labeled by 2 and 3 in the coherent interface model shown in Fig. 2 are adopted as the substitution sites for W and Mo. In order to study the partitioning behaviors of W and Mo with and without Re and Ru on the interface, the binding energies of three categories are compared, namely the cases that the central atom is Ni or Re or Ru. Then the Ni atom labeled by 2 in the pure  $\gamma$  phase are substituted with W and Mo, respectively. The next step is to substitute the Ni atom labeled by 3 in the pure  $\gamma'$  phase with W and Mo, separately. All of the binding energies of the 12 quaternary Ni–Al–Re(Ru)–W(Mo) SC superalloys interface models are included in Table 3. For the Mo addition, when the central atom is Ni, the binding energy of Mo being in the  $\gamma$  phase is lower than the case when Mo stays in the  $\gamma'$  phase, illustrating the experimental and theoretical result that Mo prefers to stay in the  $\gamma$  phase [11,12,31]. When Re and Ru substitute the central Ni atom, it is still the case that Mo in the  $\gamma$  phase is more stable than that of Mo in the  $\gamma'$  phase. This result is in accordance to the fact that Re and Ru do not affect the partitioning behavior of Mo in

the  $\gamma/\gamma'$  phases. The binding energies of W addition cases in the  $\gamma/\gamma'$  interface systems give good results too. When the central atom is Ni, the W atom partitions more strongly to  $\gamma$  phase, the reason being that  $E_b$  is  $-715.05$  eV and  $-714.80$  eV within W in the pure Ni and Ni<sub>3</sub>Al phases, respectively. This is consistent with the experimental conclusions [32]. When Re substitutes the central Ni atoms, the binding energy within W in the  $\gamma'$  phase is  $-717.10$  eV and within the  $\gamma$  phase is  $-714.54$  eV, respectively. W obviously prefers to partition into the  $\gamma'$  phase due to the lower binding energy. The binding energy decreases by a remarkable 2.30 eV when W is in the  $\gamma'$  phase within Re on the interface region. Therefore, Re not only serves as a phase stability factor for refractory element W, but also triggers the W's reverse partitioning behavior. Ru seems to have no effect on the partitioning behavior of W. The effect of Re and Ru on the partitioning behavior of W and Mo is in good agreement with the experimental result from Volek et al. [14]. It is also noticed that except for the case within W in the  $\gamma'$  phase, the Re substitution for Ni increases the binding energy of the systems, which means Re is a phase instability factor and too much of Re on the interface may precipitate as TCP phases. On the other hand, with Ru substituting for Ni, the binding energies for all the cases decrease, which illustrates the well-known fact that Ru can improve the microstructural stability. The above binding energy results give insight into the different alloying effect of Re and Ru, especially their effect on the partitioning behaviors of W and Mo to  $\gamma$  and  $\gamma'$  phases.

### 3.3.2. Mulliken population

It is well known that the Mulliken orbital population [33] can be used to describe quantitatively the charge transfer between orbitals and the charge accumulation or depletion around atoms, thus being helpful to interpret the alloying mechanism of Re and Ru to W and Mo. Table 4 lists the electron occupation numbers in the valence orbitals for the interfaces containing W or Mo in the  $\gamma$  or  $\gamma'$  phases with and without Re and Ru on the interface, respectively. It is found that for all the cases of W, the 6s orbital gains charge, while 5d and 6p orbitals lose charge. The same charge transfer behavior is found for both Ni and Re, namely charge transfers from the 4s-Ni to 3d-Ni and 4p-Ni orbitals and from the 6s-Re to 5d-Re and 6p-Re orbitals, respectively. However, it is not the case for Ru, where all the 4d-Ru, 5s-Ru, 5p-Ru orbitals obtain electron. The charge transfer behavior of this type indicates that between orbitals of Ni, Re and W exists strong hybridization, which is an alloying strengthening factor of SC superalloys. Compared to Re, the alloying strengthening mechanism of Ru is not direct through the bonding enhancement to W and the host atoms. Many experimental works support our conclusion in the present calculation [5,6,9,28]. The Mulliken population result is consistent with the above binding energy analysis. When Re substitutes Ni(1) atom corresponding to Fig. 2, the binding energy for the interface systems with W at 3 atomic site and at 2 atomic site is  $-715.98$  eV and  $-717.09$  eV, respectively, which explains the effect of Re on the reverse partitioning behavior of W. In contrast with Re, when Ru substitutes Ni(1) site in Fig. 2, the binding energies of the systems with W is little affected. It is further illustrated that the

Table 3  
The binding energy for the coherent interface systems centering at Ni, Re and Ru atoms with W(Mo) additions in the  $\gamma$  and  $\gamma'$  phases, respectively

Elements	Phase	$E_b$ free (eV)	$E_b$ Re (eV)	$E_b$ Ru (eV)
Mo	$\gamma$	$-713.62$	$-713.14$	$-714.50$
Mo	$\gamma'$	$-713.46$	$-712.97$	$-714.31$
W	$\gamma$	$-715.05$	$-714.54$	$-715.91$
W	$\gamma'$	$-714.80$	$-717.10$	$-715.62$

$E_b$  free ( $E_b$  Re,  $E_b$  Ru) denotes the binding energy of interface models shown in Fig. 2 with Ni(Re,Ru) as the central atom, while Mo or W at the 2 or 3 atomic site.

Table 4

The electron occupation number  $N_{(\text{Ni,W})}$ ,  $N_{(\text{Re,W})}$ ,  $N_{(\text{Ru,W})}$  in the valence orbitals for the  $\gamma/\gamma'$  and  $\gamma/\gamma'$ -Re and  $\gamma/\gamma'$ -Ru with W in the  $\gamma$  or  $\gamma'$  phases, respectively

Atom	Orbitals	$\gamma/\gamma'$ $N_{(\text{Ni,W})}$	$\gamma/\gamma'$ $N_{(\text{Ni,W})}$	$\gamma/\gamma'$ -Re $N_{(\text{Re,W})}$	$\gamma/\gamma'$ -Re $N_{(\text{Re,W})}$	$\gamma/\gamma'$ -Ru $N_{(\text{Ru,W})}$	$\gamma/\gamma'$ -Ru $N_{(\text{Ru,W})}$
W(2)	5d		4.942		4.907		4.911
	6s		1.128		1.102		1.109
	6p		0.967		0.965		0.972
	$Q$		+1.037		+0.974		+0.992
Ni(Re,Ru)(1)	3(5,4)d	8.609	8.608	5.955	5.978	7.171	7.180
	4(6,5)s	1.168	1.168	1.170	1.131	1.043	1.103
	4(6,5)p	0.668	0.679	0.963	1.009	0.741	0.769
	$Q$	+0.445	+0.445	+1.088	+1.118	+0.955	+0.962
W(3)	5d	4.317		4.269		4.256	
	6s	0.920		0.826		0.872	
	6p	0.818		0.837		0.854	
	$Q$	+0.055		-0.068		-0.018	

Here  $Q = N - Z_{\text{val}}$ , where  $Z_{\text{val}}$  is the standard number of valence electrons per atom. The Arabic numerals in W(2), Ni(Re,Ru)(1) and W(3) correspond to those in Fig. 2.

direct bonding between Ru and W is weaker than that of Re and W.

From the view of charge accumulation or depletion around atoms, when Re and Ru substitute Ni(1), the W(2) atom gains approximately 1e charge; on the other hand, W(3) gains or loses very little charge. In more detail, when Re substitutes Ni(1), more charge transfers from 6s-W to 4d-W to compensate for the

little charge depletion of W(2) and W(3). Re itself gains some 1.1e electrons, which transfer from 6s-Re to 5d-Re, resulting in Re-d/W-d hybridization and further enhancing the bonding across interface. As a comparison, a single Ru atom substituting for Ni(1) obtains less charge than Re does, especially it is found that all the 4d, 5s, 5p orbitals of Ru gain electrons. This difference affects the bonding properties of Ru-d/W-d, unluckily

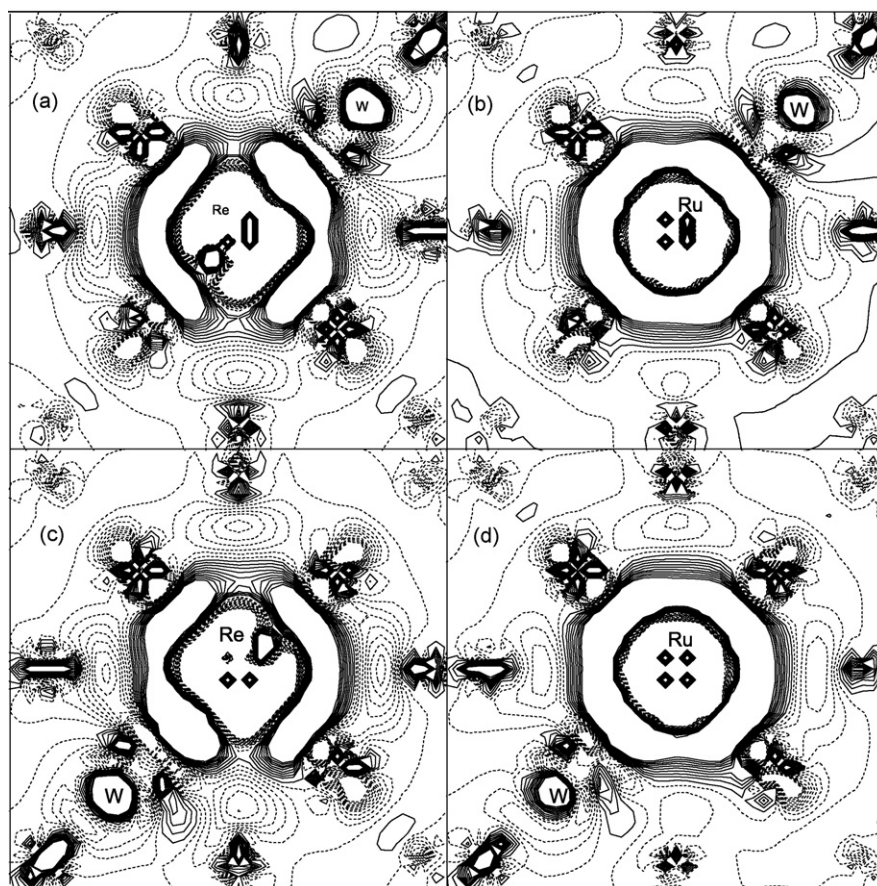


Fig. 4. The electron density difference on the (100) plane across the interface. (a) Ni-Al-Re-W with W in the  $\gamma'$  phase, (b) Ni-Al-Ru-W with W in the  $\gamma'$  phase, (c) Ni-Al-Re-W with W in the  $\gamma$  phase and (d) Ni-Al-Ru-W with W in the  $\gamma$  phase. The atomic sites correspond to those in Fig. 2. The contour spacing is 0.001 e a.u.<sup>-3</sup>. Solid lines and dashed lines correspond to the increased and the decreased charge density, respectively.

weakening the interaction between the  $\gamma$  and  $\gamma'$  phases. Based on the above discussion, the different alloying strengthening mechanism of Re and Ru can be understood. The way of Re induced enhancement originates from the direct bonding between Re and the host W or Ni atoms, whereas the strengthening mechanism of Ru is indirect, by decreasing the binding energy and thereby improving the microstructural stability.

### 3.3.3. Charge difference redistribution and partial density of states

In order to understand deeply the alloying mechanisms of Re and Ru on the refractory element W, the charge redistribution induced by Re and Ru substitution for Ni(1) on (100) planes across the interface are plotted, which contains atomic sites labeled by 1, 2 and 3 in Fig. 2. The charge density differences are plotted in Fig. 4. For the interface system with W(2) or W(3), when Re(1) replaces Ni(1), the charge difference can be defined as:

$$\Delta\rho = \rho(\text{Ni}_{67}\text{Al}_{18}\text{ReW}) - \rho_{\text{free}}(\text{Ni}_{67}\text{Al}_{18}\text{ReW}) - \rho(\text{Ni}_{68}\text{Al}_{18}\text{W}) + \rho_{\text{free}}(\text{Ni}_{68}\text{Al}_{18}\text{W}) \quad (2)$$

Here  $\rho(\text{Ni}_{67}\text{Al}_{18}\text{ReW})$  is the charge density of the cluster interface model shown in Fig. 2 with Re at the center (Re substitute the central Ni atom); system with W(2) is in the  $\gamma'$  phase or W(3) in the  $\gamma$  phase. For the quaternary interface Ni–Al–Ru–W, the similar definition can be introduced:

$$\Delta\rho = \rho(\text{Ni}_{67}\text{Al}_{18}\text{RuW}) - \rho_{\text{free}}(\text{Ni}_{67}\text{Al}_{18}\text{RuW}) - \rho(\text{Ni}_{68}\text{Al}_{18}\text{W}) + \rho_{\text{free}}(\text{Ni}_{68}\text{Al}_{18}\text{W}) \quad (3)$$

As seen from (a) and (c) in Fig. 4, charge correction regions due to the electron accumulation appear around the Re atom and the NN W and Ni atoms. This indicates that the bonding for Re(1) and its NNs is stronger than that for Ni(1) and its NNs when Re(1) substitutes the central Ni(1) atom, which reflects enhanced interactions between Re(1) and its NN W and Ni atoms in the quaternary  $\gamma/\gamma'$  interface. Particularly, the interaction across the interface is enhanced according to the charge accumulation across phase boundary. No matter in which phases W is, the charge accumulates between Re and W due to Re(1)'s substitution for Ni(1), which results from a fact that Re is a alloying strengthening factor for W either in the  $\gamma$  or  $\gamma'$  phases.

In contrast with Re, the charge correction induced by Ru substitution are also plotted, as shown in (b) and (d) of Fig. 4. The charge redistribution takes on a ring-like shape, which is different from the shuttle-like charge distribution induced by Re. This type of charge redistribution is not as good as Re for the enhancement of interactions across the interface. But it is noticed that the charge density of NNs of Ru(1) including both W and Ni themselves is apparently increased. The charge redistribution is consistent with the conclusions got in the binding energy and the Mulliken population analysis. These results provide explanation for the different alloying strengthening mechanisms of Re and Ru.

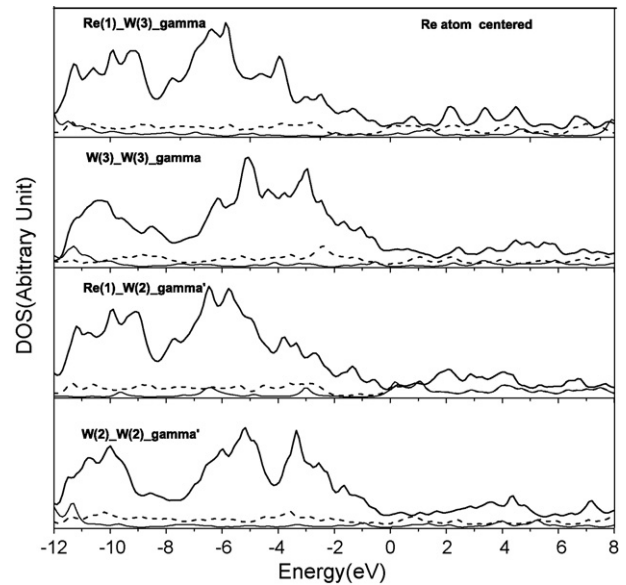


Fig. 5. The atomic partial density of states in the Ni–Al–Re(1)–W(2,3) system. Re(1)–W(2)–gamma etc. correspond to the PDOS of atom Re(1), while W(2) element is in the  $\gamma$  phase shown in Fig. 2. The thick solid lines, thin solid lines and dashed lines denotes d, s, p electronic states, respectively. The Fermi level is shifted to zero.

Besides charge difference, we have calculated the partial density of states (PDOS) by means of Lorenz broadening scheme. PDOS for the central Re(1) or Ru(1) atoms, the NN W(2) and W(3) atoms of the four different systems are shown in Figs. 5 and 6. Re(1)–W(2)–gamma stands for the case when Re substitutes the central Ni(1) atom, and W replaces the Ni(2) atom shown in Fig. 2, and so on. It is easy to understand that the interaction between Re, Ru and W is mainly by the hybridization

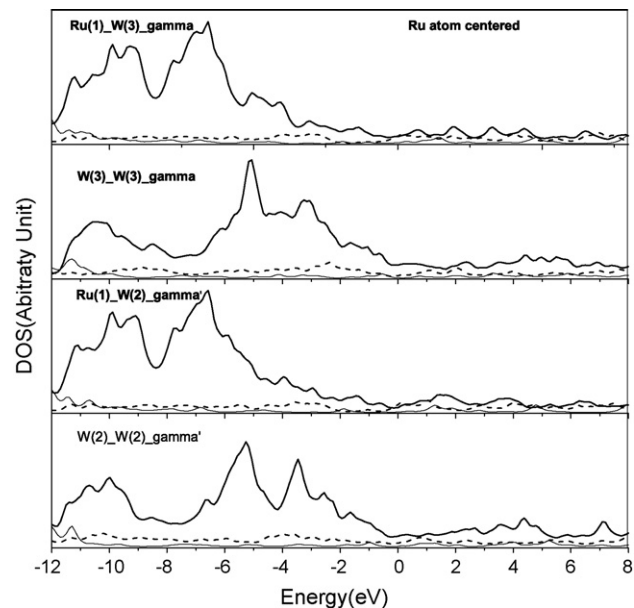


Fig. 6. The atomic partial density of states in the Ni–Al–Ru(1)–W(2,3) system. Ru(1)–W(2)–gamma etc. correspond to the PDOS of atom Ru(1), while W(2) element is in the  $\gamma$  phase shown in Fig. 2. The thick solid lines, thin solid lines and dashed lines denote d, s, p electronic states, respectively. The Fermi level is shifted to zero.



of d orbitals, because most of their valence electrons are from the d orbitals. It can be seen from Figs. 5 and 6 that there exists strong hybridization between Re 5d-W 5d, Ru 4d-W 5d, which results in the strong bonding between Re-W and Ru-W. It is interesting to notice that two obvious resonant peaks appear 5.5 eV and 10 eV below the Fermi energy in Fig. 5. As a comparison, for the PDOS curves of Ru(1) and W(2,3) shown in Fig. 6, the resonant peak locating at  $-10$  eV still exists, however, the one in  $-5.5$  eV disappears, as a result from the fact that the isolate peak of Ru shift by about 1 eV to the lower energy. This difference from the interaction between Re and W makes the hybridization of Ru d-W d weaker. This is consistent with the above conclusion from the binding energy and so on. The peaks of Ru-d orbitals shift to lower energy compared with the orbital energy of Re, which explains that Ru can decrease the binding energy of the  $\gamma/\gamma'$  interface systems, further improving the microstructural stability. Once again, the calculations of PDOS provide us the different alloying strengthening mechanisms of Re and Ru.

#### 4. Summary

In sum, the following conclusions can be reached:

1. The site preference of Re and Ru on the  $\gamma/\gamma'$  interface is determined by the DMol3 calculation. The calculated transfer energies show that both Re and Ru prefer to occupy a Ni site on the Ni–Ni<sub>3</sub>Al interface. When Re and Ru replace the Al atom, the binding energies of the coherent interface systems are decreased. However, when Re or Ru substitutes a Ni atom on the Ni–Ni<sub>3</sub>Al interface, only the Ru can lower the binding energy and further improve the microstructural stability. This is consistent with the experimental result that Re is a phase instability factor that may result in the precipitation of TCP phases, while Ru is added to the fourth generation Ni-based SC superalloys as a phase stability factor.
2. Re remarkably affects the partitioning behavior of W between the  $\gamma$  and  $\gamma'$  phases. With the Re addition, W partitions more strongly to the  $\gamma'$  phases. Therefore with higher levels of refractory elements in the  $\gamma'$  phase, susceptibility to TCP precipitation in the  $\gamma$  phase was induced, which is beneficial for the resistance to creep within high-temperature. However, Re does not affect the reverse the partitioning behavior of Mo. Our work also shown the experimental result from Volek et al. [14] that Ru has no effect on the partitioning behavior of both W and Mo.
3. Our calculation result for the bonding energy, Mulliken population, charge difference and partial density of states consistently elucidate the different alloying strengthening mechanism of Re and Ru. The strengthening of alloy by the Re addition is direct, by enhancing the interaction between

Re and its nearest neighbors. In contrast, the strengthening effect of Ru is indirect, by lowering the binding energy of the system, resulting in the improvement of microstructural stability.

#### Acknowledgement

This work is supported by “973 Project” from the Ministry of Science and Technology of China (Grant No. 2006CB605102).

#### References

- [1] I.L. Mrkin, O.D. Kanchev, *Met. Sci. Heat Treat.* 1–2 (1967) 10.
- [2] A. Giamei, D.L. Anton, *Met. Trans. A* 16A (1997) 1985.
- [3] A.D. Cetel, D.N. Duhal, *Superalloys, The Minerals, Metals and Materials Society*, 1992, p. 287.
- [4] B.D. Bryskin, *Rhenium and Rhenium Alloys, The Minerals, Metals and Materials Society*, 1997, p. 731.
- [5] S. Walston, A. Celal, et al., *Superalloys* (2004) 15–24.
- [6] A.C. Yeh, S. Tin, *Metal. Mater. Trans. A* 37A (2006) 2621.
- [7] A.F. Voter, S.P. Chen, in: R.W. Siegel, et al. (Eds.), *MRS Symposia Proceedings No. 82, Materials Research Society, Pittsburgh*, 1987, p. 175.
- [8] I.L. Mirkin, O.D. Kanchev, *Met. Sci. Heat Treatment* 10 (1967) 1–2.
- [9] Q. Feng, J.F. Mansfield, T.M. Pollock, *Metall. Mater. Trans. A* 37 (2006) 2927.
- [10] C. Vernault, et al., *Met. Mater. Soc.* (2000) 829.
- [11] U. Hemmersmeier, M. Feller-Kniepmeier, *Mater. Sci. Eng. A* 248 (1998) 87–97.
- [12] C. Schulze, M. Feller-Kniepmeier, *Mater. Sci. Eng. A* 281 (2000) 204–212.
- [13] P. Caron, High solvus new generation nickel-based superalloys for single crystal turbine blade applications, *superalloys* (2000) 737–746.
- [14] A. Volek, et al., *Scrip. Mater.* 52 (2005) 141–145.
- [15] S.-Y. Wang, C.-Y. Wang, et al., *Phys. Rev. B* 65 (2001) 035101.
- [16] A.P. Ofori, C.J. Humphreys, S. Tin, et al., *Superalloys* (2004) 787–794.
- [17] A.P. Ofori, C.J. Rossouw, C.J. Humphreys, *Acta Mater.* 53 (2005) 97–110.
- [18] C.Y. Geng, C.Y. Wang, et al., *Acta Mater.* 52 (2004) 5427–5433.
- [19] S. Raju, E. Mohandas, V.S. Raghunathan, *Scrip. Mater.* 34 (1996) 1785.
- [20] J. Shen, Y. Wang, N.X. Chen, Y. Wu, *Prog. Nat. Sci.* 10 (2000) 457.
- [21] B. Delley, *J. Chem. Phys.* 92 (1990) 508.
- [22] B. Delley, *J. Chem. Phys.* 94 (1990) 7245.
- [23] M. Dolg, U. Wedig, H. Stoll, H. Preuss, *J. Chem. Phys.* 86 (1987) 866.
- [24] A. Bergner, M. Dolg, W. Kuechle, H. Stoll, H. Preuss, *Mol. Phys.* 80 (1993) 1431.
- [25] J.P. Perdew, K. Burke, M. Ernzerhof, *Phys. Rev. Lett.* 78 (1997) 1396.
- [26] J.H. Xu, T. Oguchi, A.J. Freeman, *Phys. Rev. B* 37 (1998) 6757.
- [27] R. Darolia, D.F. Lahrman, R.D. Field, *Superalloys* (1988) 255–264.
- [28] A. Sato, et al., *Scrip. Mater.* 54 (2006) 1679.
- [29] A.V. Ruban, H.L. Skriver, *Phys. Rev. B* 55 (1997) 856.
- [30] P. Peng, et al., *Comp. Mater. Sci.* 38 (2006) 354.
- [31] C. Schulze, M. Feller-Kniepmeier, *Scrip. Mater.* 44 (2001) 731.
- [32] D. Blavette, P. Caron, T. Khan, in: *Proceedings of the 6th International Symposium on Superalloys, Warrendale*, 1988, pp. 305–314.
- [33] R.S. Mulliken, *J. Chem. Phys.* 23 (1955) 1833.
- [34] K.S. O'Hara, W.S. Walston, E.W. Ross, R. Darolia, US Patent NO.5, 482, 789, General Electric Company (1996).